Supporting Information for

Conversion of CO_2 into Porous Metal-Organic Frameworks Monoliths

Kanchana Sotho,[a] Kentaro Kadota,*[b] Takuya Kurihara,[c] Thanakorn Tiyawarakul,[a] Hiroki Yamada,[d] Kanokwan Kongpatpanich,[a] and Satoshi Horike*[a,b,e]

[a] Department of Materials Science and Engineering, School of Molecular Science and Engineering, Vidyasirimedhi Institute of Science and Technology, Rayong 21210, Thailand
[b] Department of Chemistry, Graduate School of Science, Kyoto University, Kitashirakawa-Oiwakecho, Sakyo-ku, Kyoto 606-8502, Japan
[c] Division of Material Chemistry, Graduate School of Natural Science and Technology, Kanazawa University, Kanazawa, Ishikawa 920-1192, Japan
[d] Diffraction and Scattering Division, Japan Synchrotron Radiation Research Institute (JASRI), Sayo, Hyogo 679-5198, Japan
[e] Institute for Integrated Cell-Material Sciences, Institute for Advanced Study, Kyoto University, Yoshida-Honmachi, Sakyo-ku, Kyoto 606-8501, Japan

Table of Contents

Materials

All chemicals and solvents used in the synthesis were reagents for synthesis grade. Aluminum nitrate nonahydrate, Cerium(III) nitrate hexahydrate, deuterated dimethyl sulfoxide (DMSO-d_6), deuterium chloride (DCl), deuterochloroform ($CDCl_3$), styrene oxide (SO) and ethanol (EtOH) were purchased from Sigma-Aldrich. Gallium(III) nitrate hydrate was purchased from Thermo Scientific. Anhydrous acetonitrile (MeCN) and anhydrous methanol (MeOH) were purchased from Alfa Aesar and Fisher Chemicals respectively. Sodium borohydride was purchased from DAEJUNG chemicals. Epichlorohydrin (ECH) and tetrabutylammonium bromide (TBAB) were purchased from TCI chemicals. All chemicals and solvents were used without further purification.

Characterizations

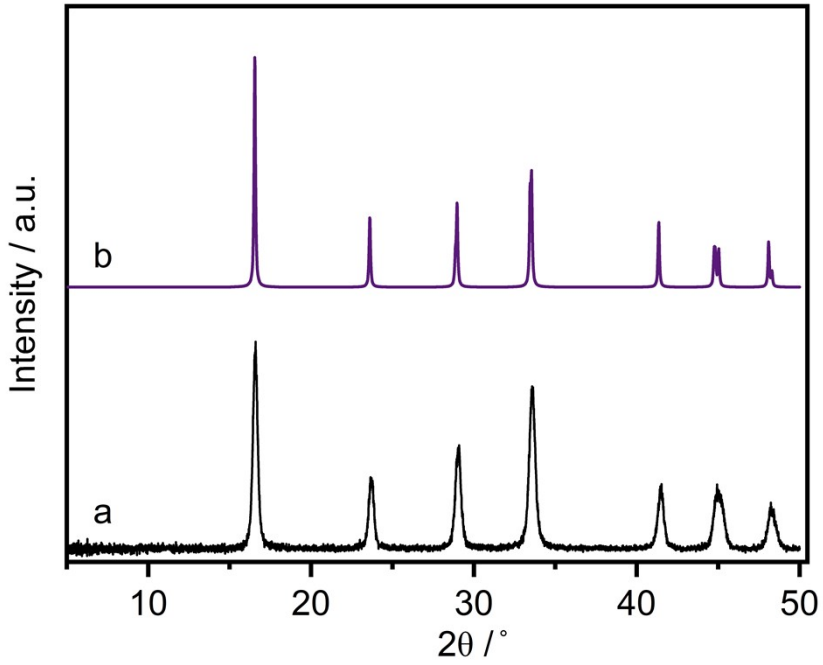

Figure S1. PXRD patterns of (a) **Ce-CO_2** and (b) $Ce(OHCO)_3$.[1]

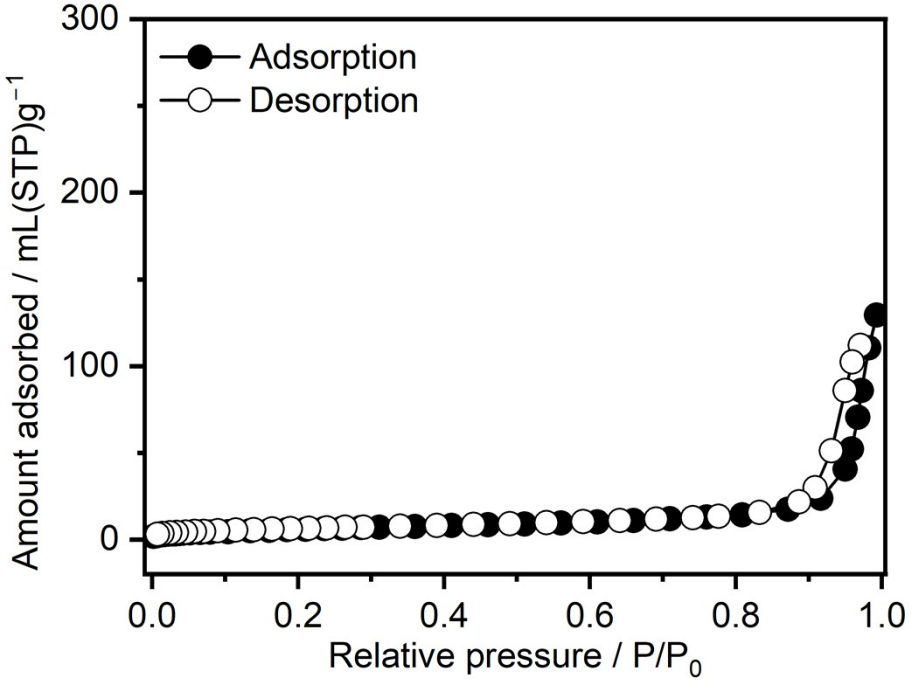

Figure S2. N_2 adsorption isotherm of **Ce-CO_2** at 77 K.

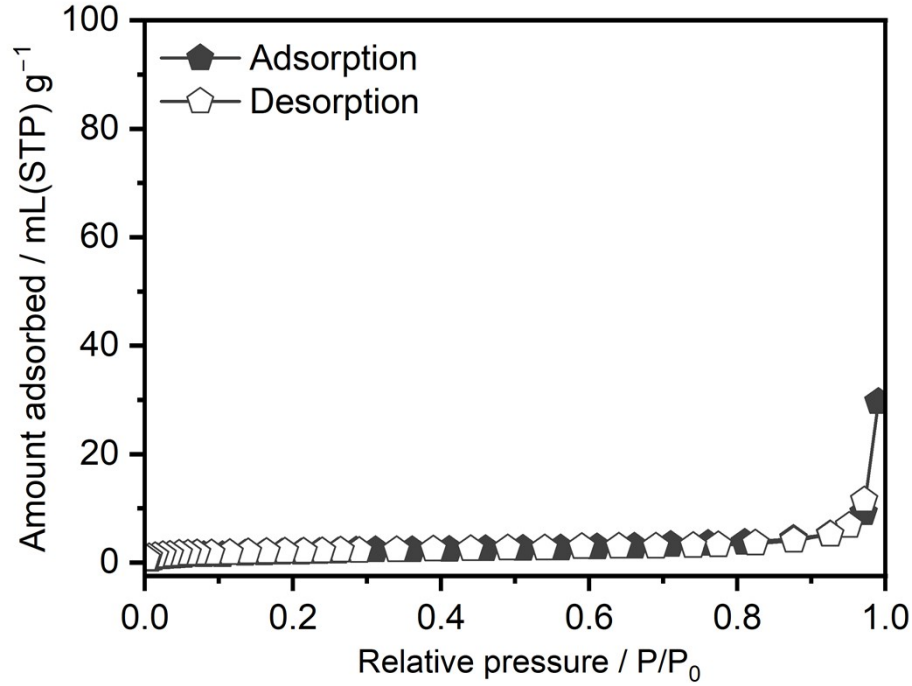

Figure S3. N_2 adsorption isotherm of **Al-CO_2** synthesized in MeCN/EtOH at 77 K

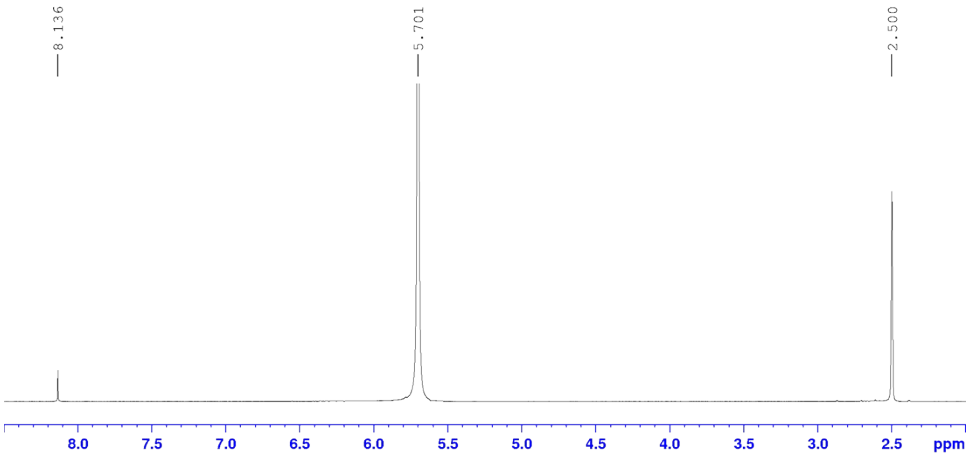

Figure S4. Acid digested ^{1}H NMR spectrum of **Al-CO$_2$** synthesized in MeCN/EtOH.

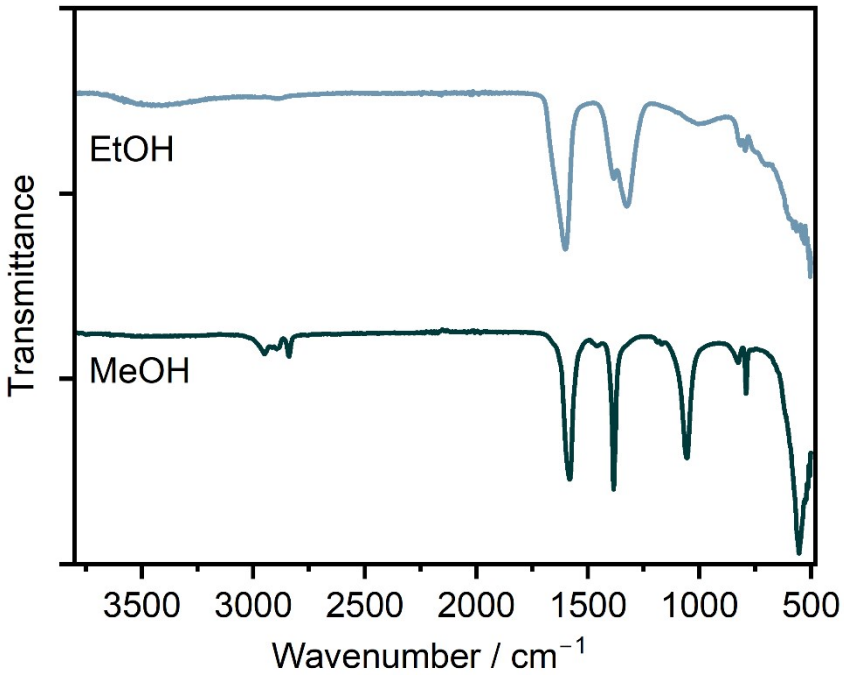

Figure S5. FT-IR spectra of **Al-CO$_2$** synthesized in MeCN/MeOH and MeCN/EtOH.

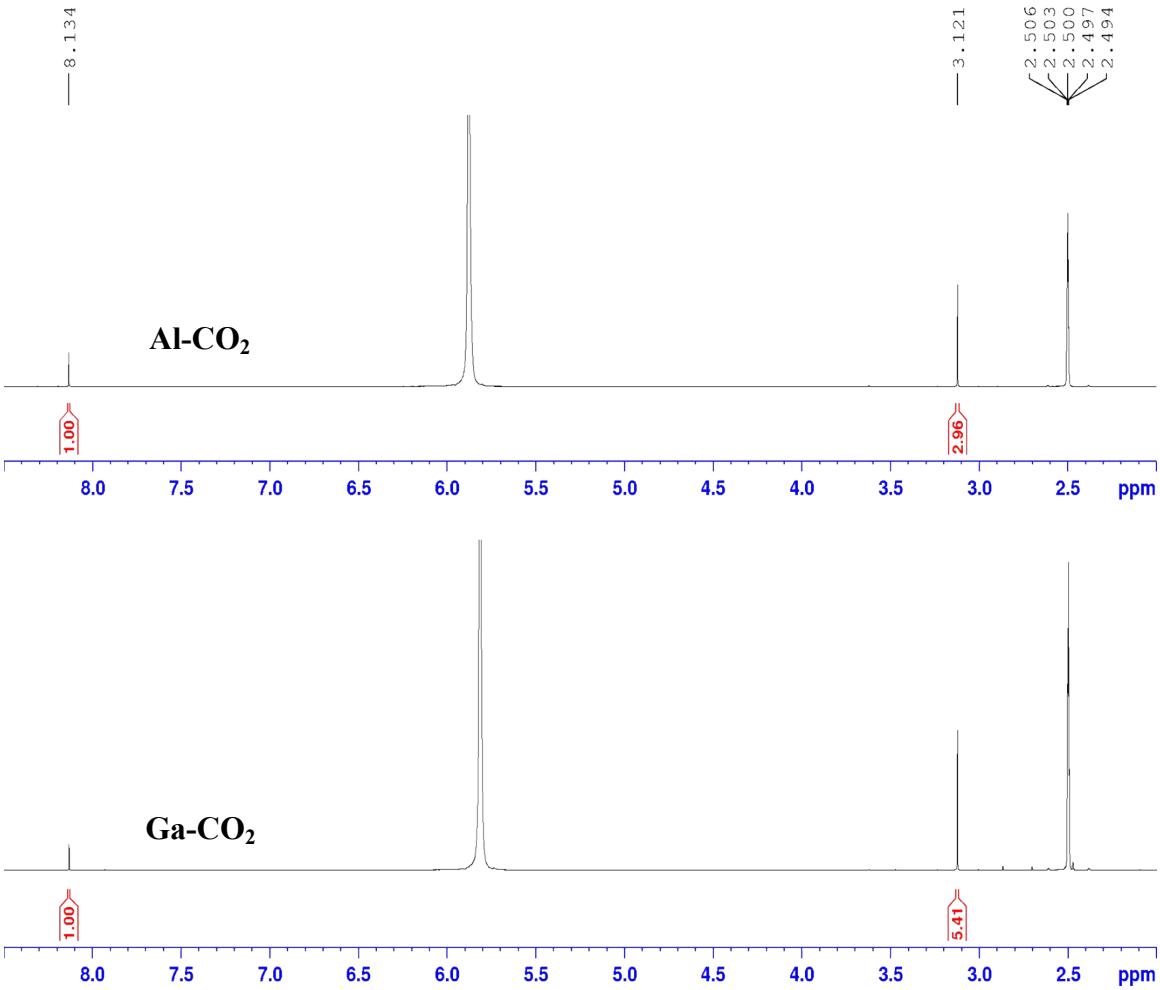

Figure S6. Acid-digested ^{1}H NMR spectra of **Al-CO$_2$** and **Ga-CO$_2$**.

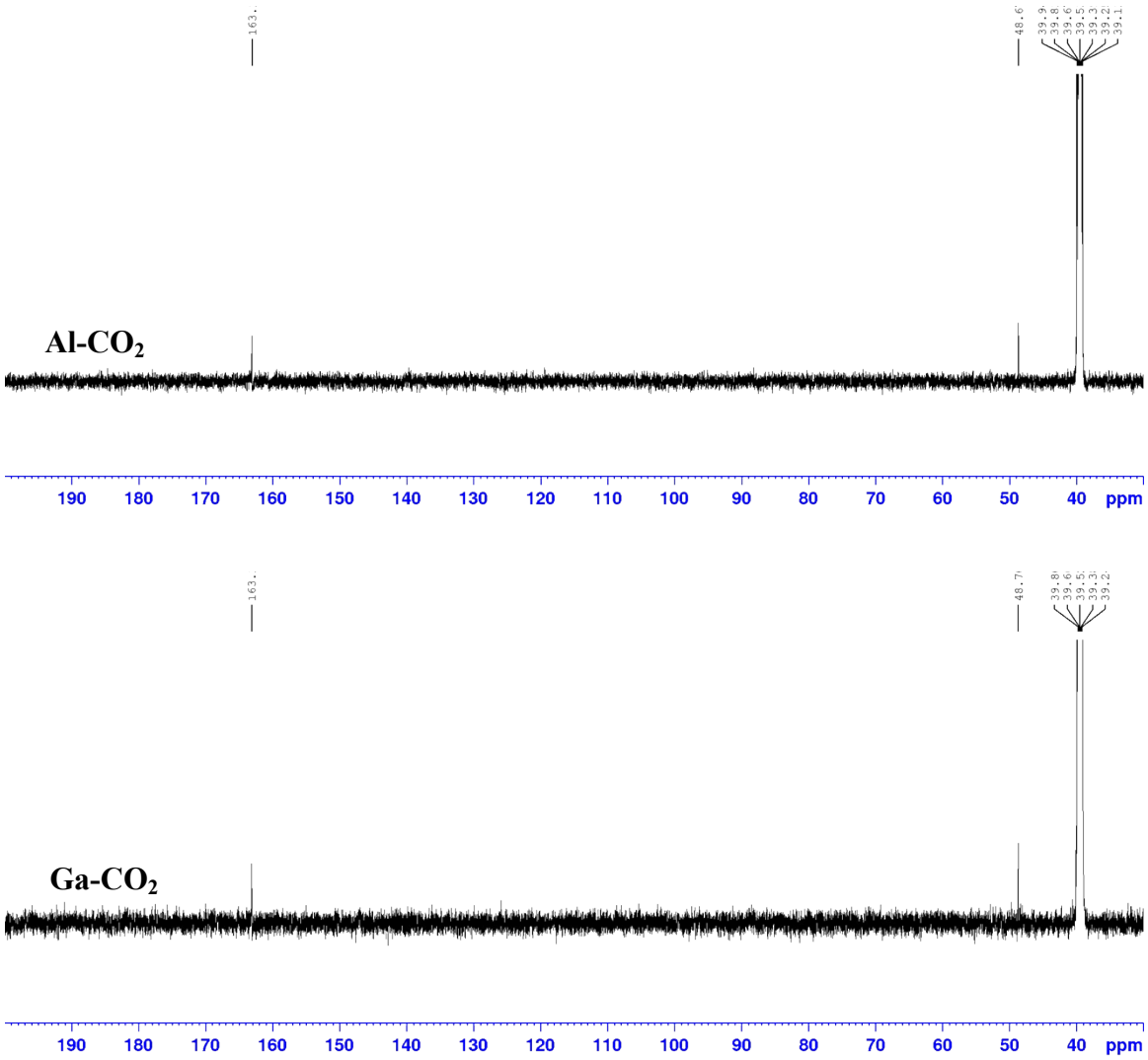

Figure S7. Acid-digested ^{13}C NMR spectra of **Al-CO_2** and **Ga-CO_2**.

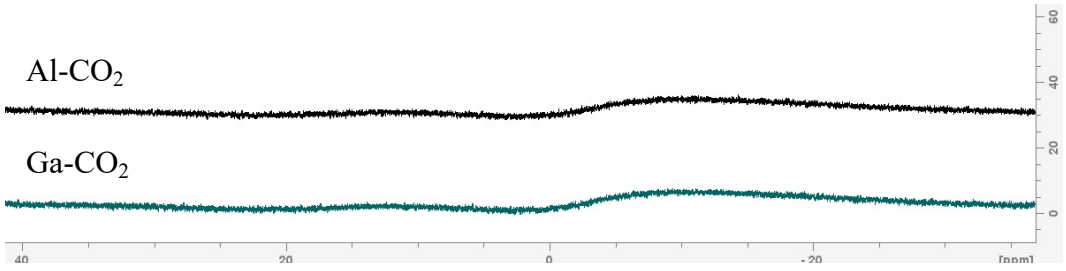

Figure S8. Acid-digested ^{11}B NMR spectra of **Al-CO_2** and **Ga-CO_2**.

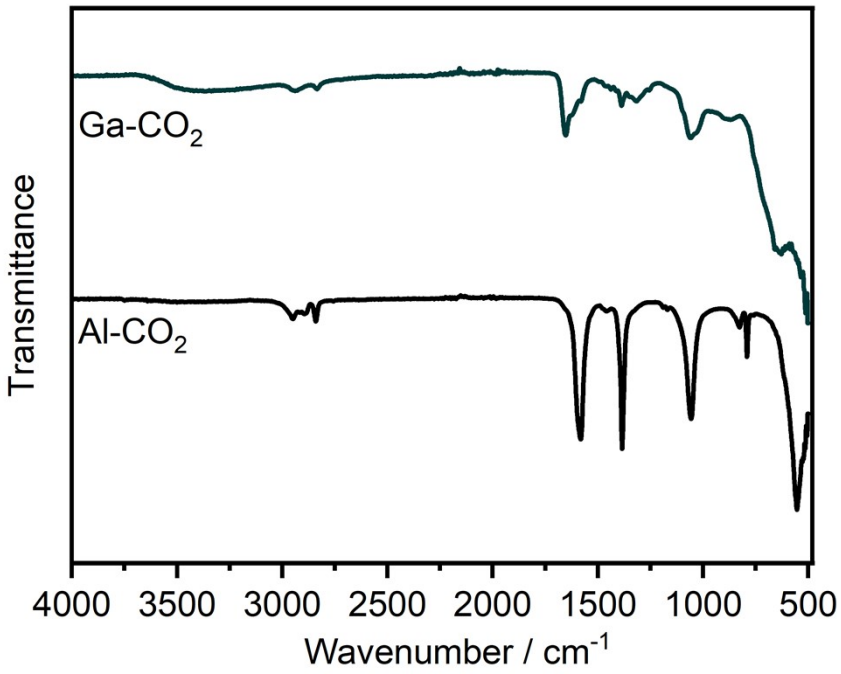

Figure S9. FT-IR spectra of **Al-CO_2** and **Ga-CO_2**.

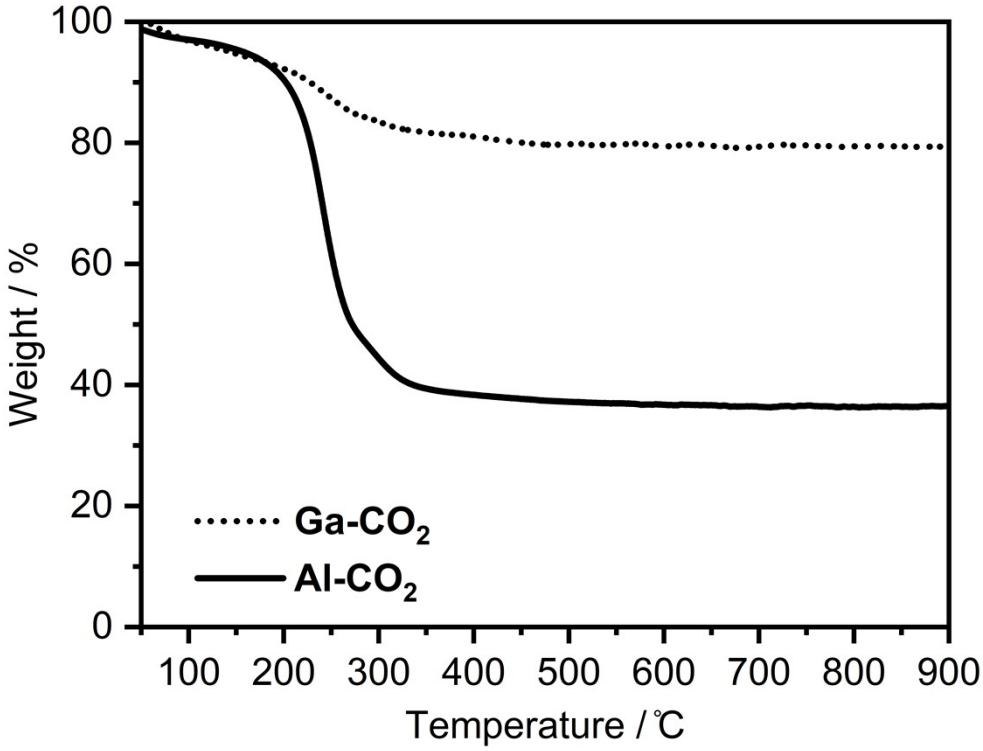

Figure S10. TGA curves of **Al-CO_2** and **Ga-CO_2** under air.

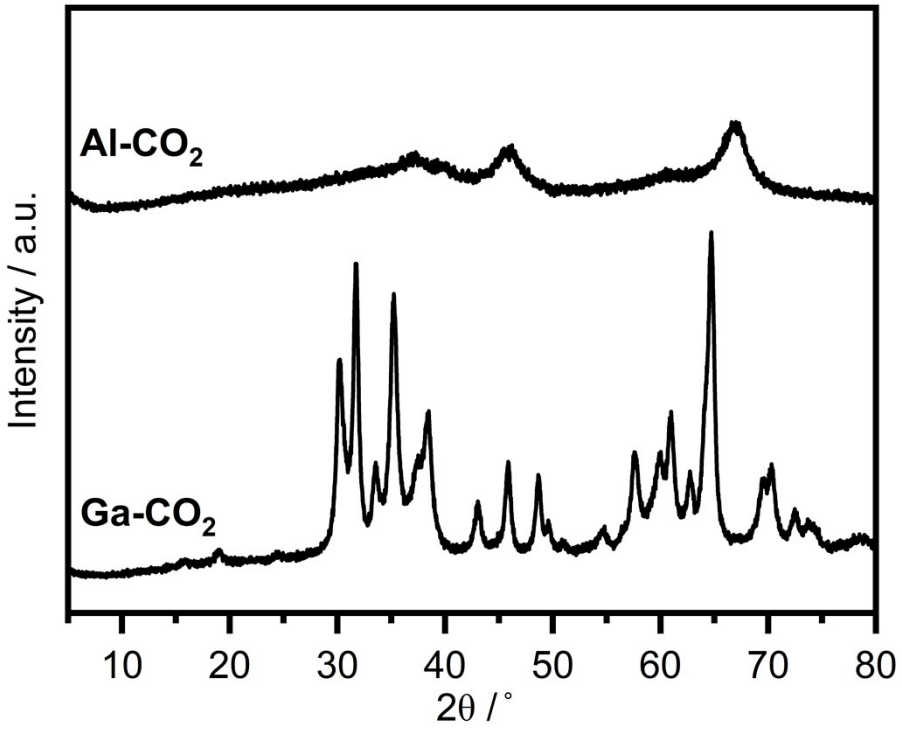

Figure S11. PXRD patterns of **Al-CO_2** and **Ga-CO_2** residues after pyrolysis. Residual metal mass was calculated by recalculating Al from Al_2O_3 (52.9 wt%) and recalculating Ga from Ga_2O_3 (74.4 wt%). The PXRD of **Al-CO_2** and **Ga-CO_2** residues match with Al_2O_3[2] and Ga_2O_3.[3]

Table S1. Elemental analysis of **Al-CO_2** and **Ga-CO_2**.

Sample	Elemental analysis (%)[a]			Metal content (%)[b]
	C	H	N	
Experimental Al-CO_2	22.3 ± 1.2	4.6 ± 0.2	0.1 ± 0.1	19.3
$Al_2(OCHO)_3(OMe)_3$	25.5*	4.3*	0*	19.1*
Experimental Ga-CO_2	5.8 ± 0.1	1.9 ± 0.1	0.5 ± 0.0	59.1
$Ga_2O_{1.8}(OHCO)_{0.5}(OMe)_{0.9}(OH)$	7.1*	1.8*	0*	59.2*

[a] Results of CHN element analysis, [b]Calculated by TGA under air.
* Calculated

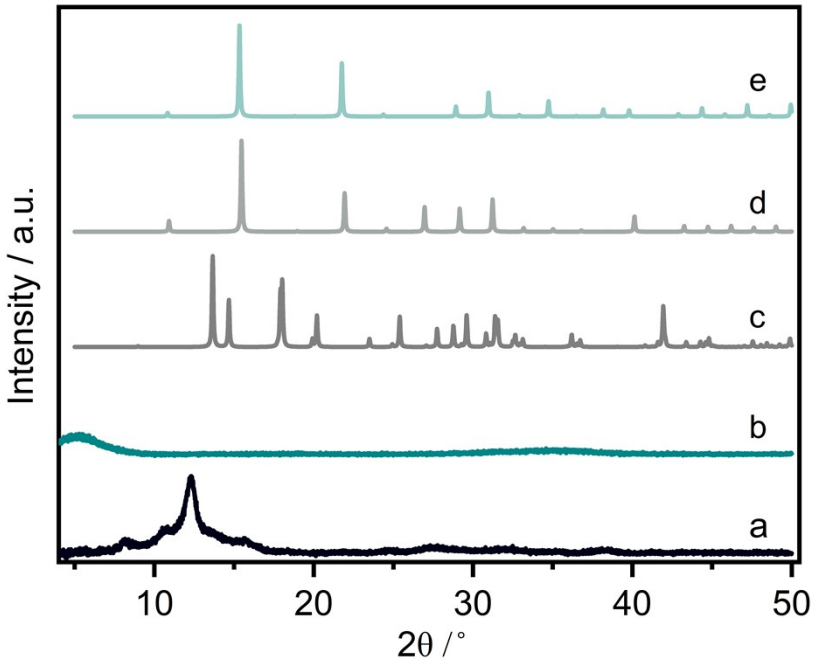

Figure S12. PXRD patterns of (a) **Al-CO_2** and (b) **Ga-CO_2** compared with simulated (c) $Al(OH)(OCHO)_2$,[4] (d) $Al(OCHO)_3$[5] and (e) $Ga(OCHO)_3$.[5]

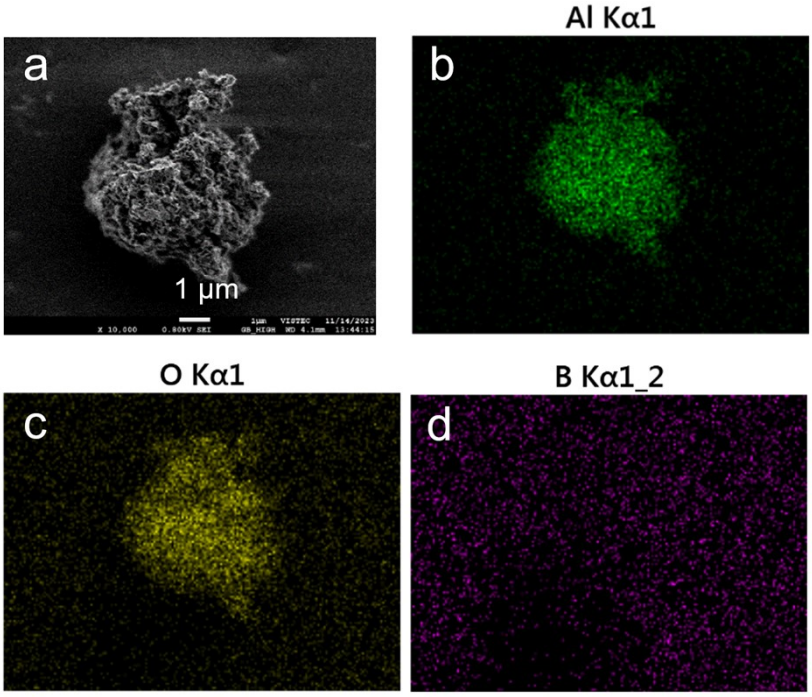

Figure S13. (a) SEM images and EDX mapping of **Al-CO_2** for (b) Al, (c) O and (d) B.

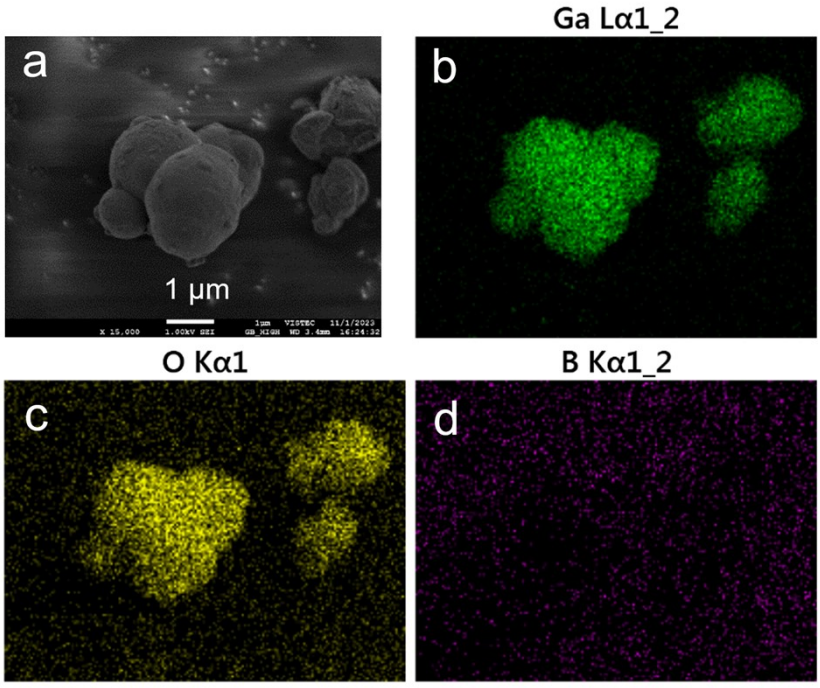

Figure S14. (a) SEM images and EDX mapping of **Ga-CO_2** for (b) Ga, (c) O and (d) B.

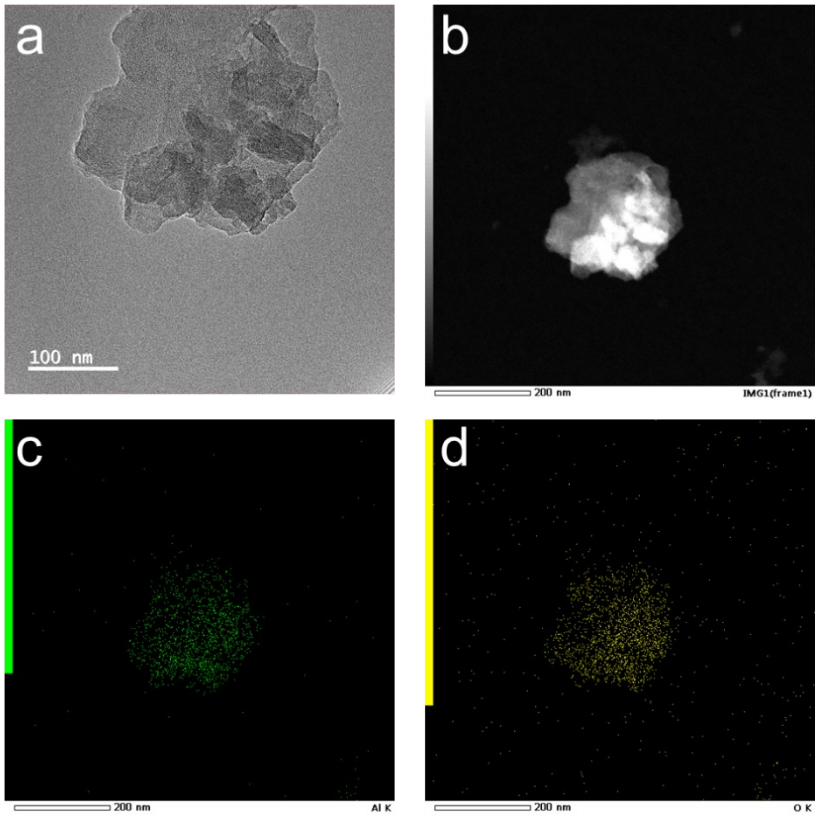

Figure S15. (a) TEM image and (b) TEM-EDS images of **Al-CO_2** for (c) Al and (d) O.

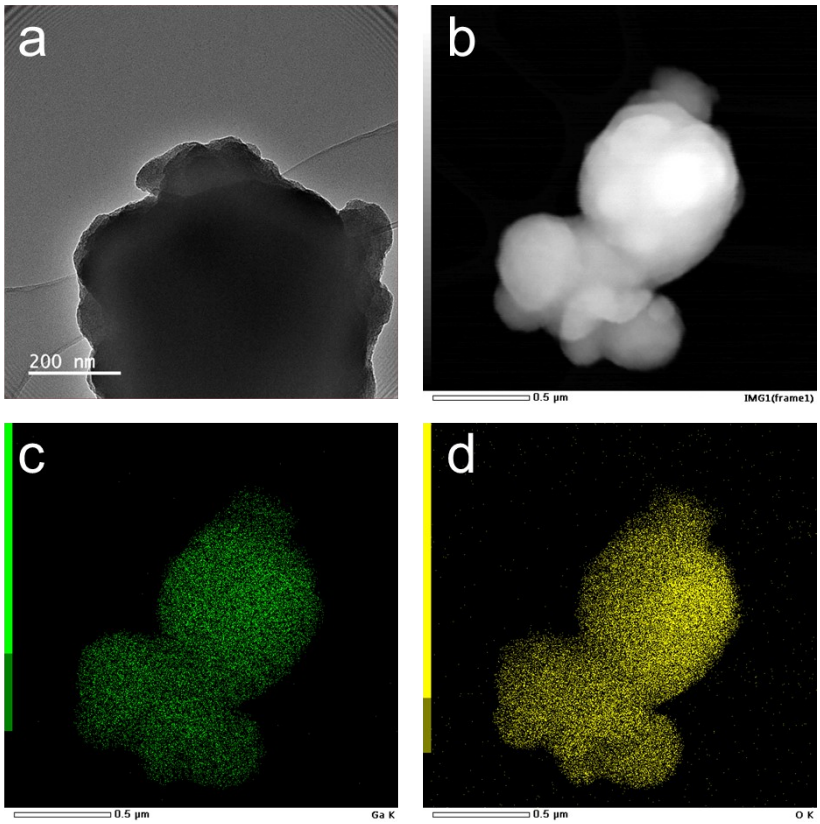

Figure S16. (a) TEM image and (b) TEM-EDS images of **Ga-CO$_2$** for (c) Ga and (d) O.

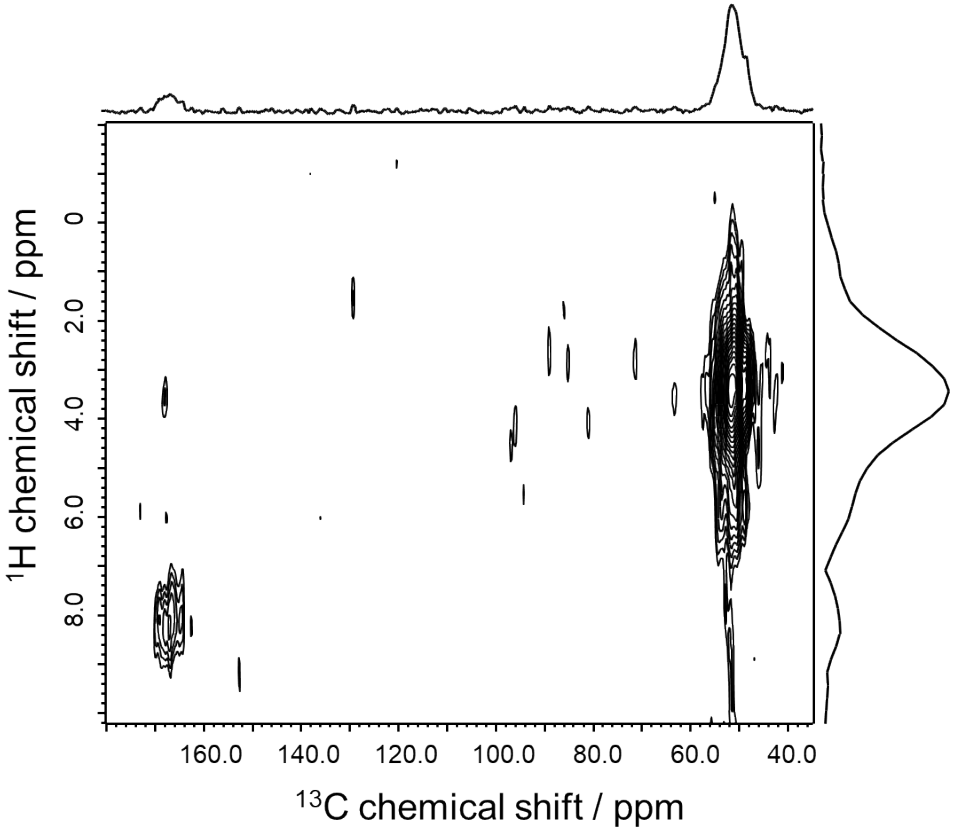

Figure S17. ^{1}H-^{13}C CP-HETCOR NMR spectra of **Ga-CO$_2$**.

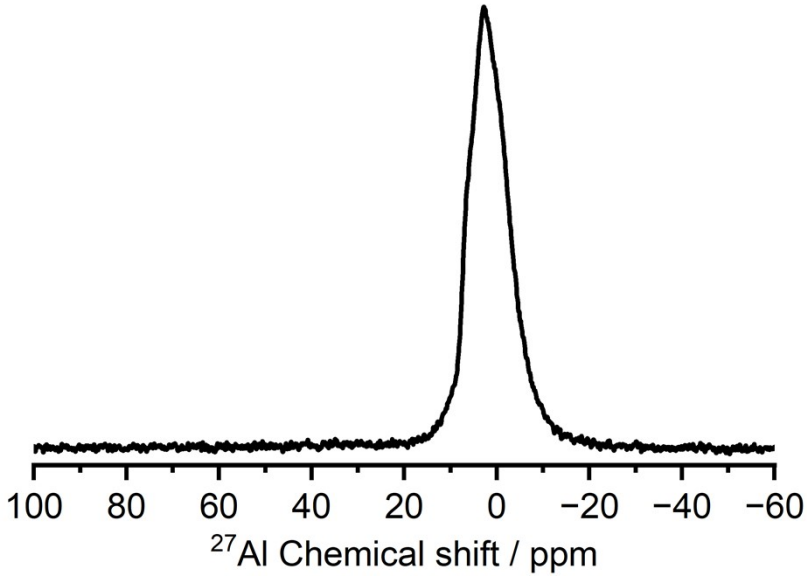

Figure S18. ^{27}Al MAS NMR spectrum of **Al-CO_2**.

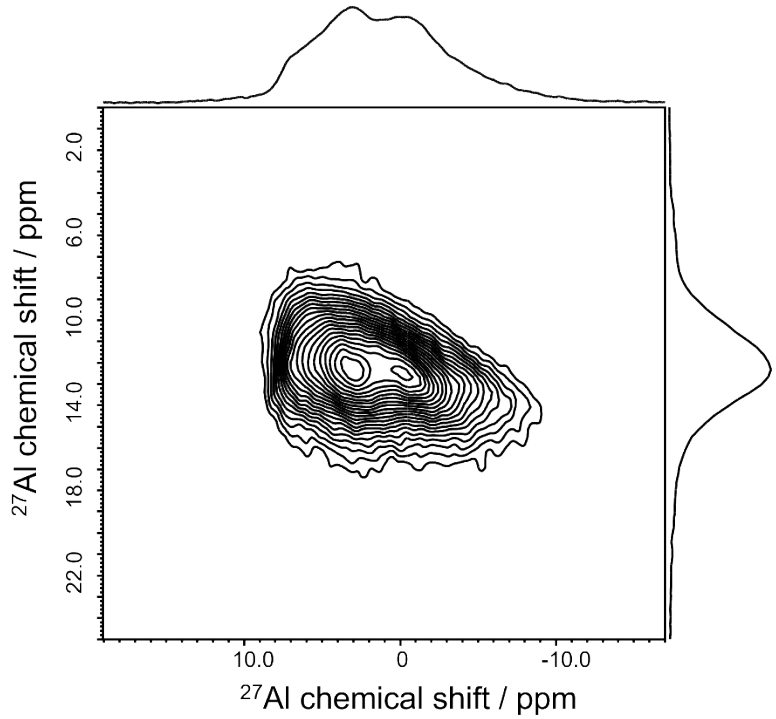

Figure S19. ^{27}Al z-filter 3QMAS spectrum of **Al-CO_2** processed by a shearing transformation. The 1D spectrum sliced at 12.31 ppm in the isotropic dimension is displayed in Figure 2C in the main text.

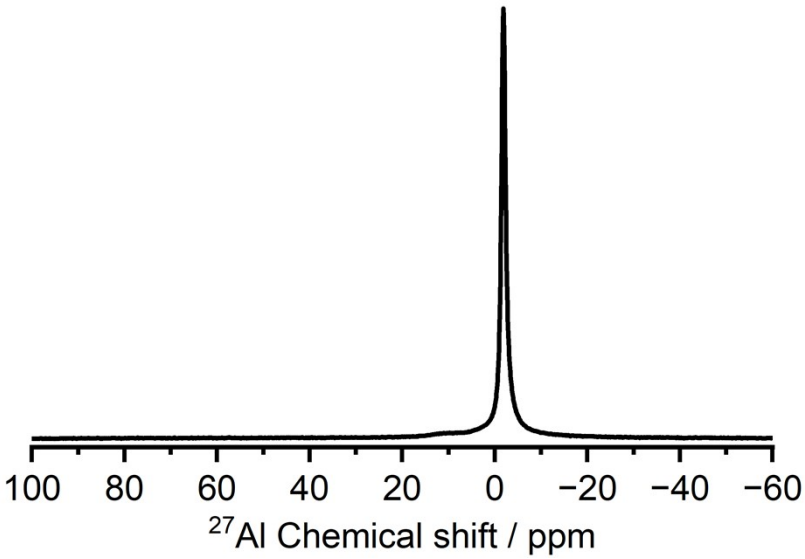

Figure S20. ^{27}Al MAS NMR spectrum of $[Al(OCHO)_3]$.

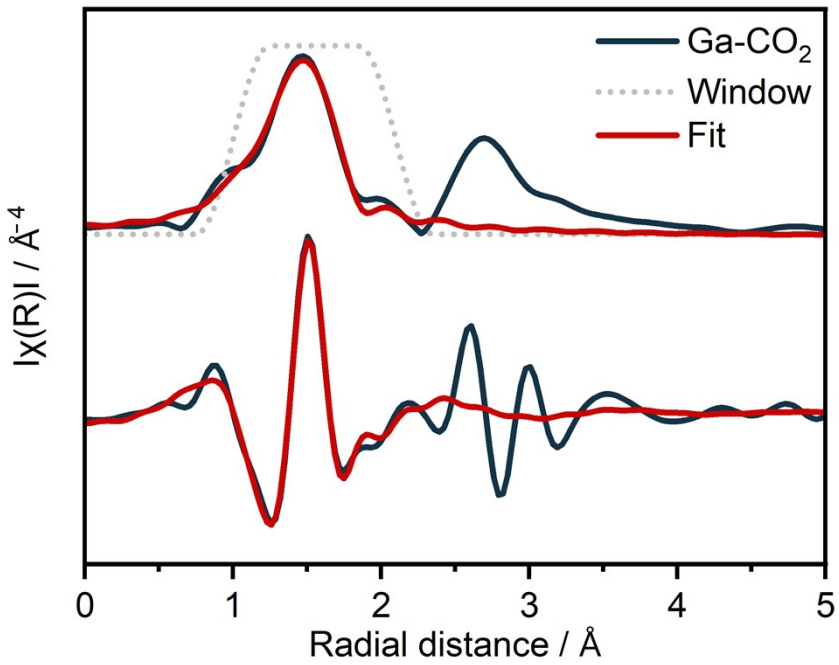

Figure S21. EXAFS spectrum (black) and fitting (red) of **Ga-CO_2**. The magnitude (top) and real component (bottom) of Fourier transformation.

Table S2. Results of the curve-fit parameters executed on the k^3-weighted FT-EXAFS spectra of **Ga-CO_2**.

Path	N	EXAFS (Å)	σ^2 (Å^2)	R-factor
Ga-O	5.6 ± 0.6	1.93	0.010	0.005

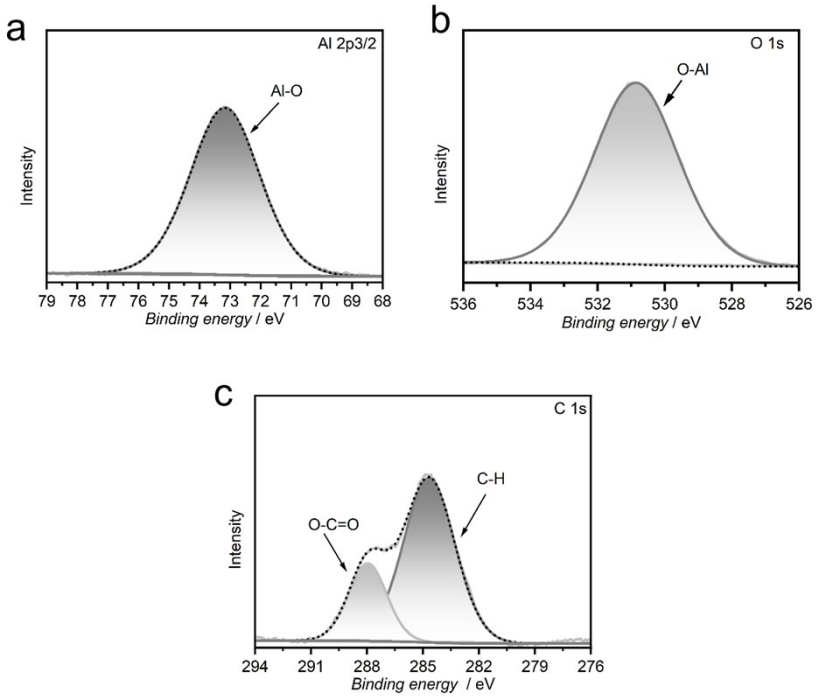

Figure S22. XPS spectra of **Al-CO_2,** (a) Al $2p_{3/2}$, (b) O 1s and (c) C 1s.

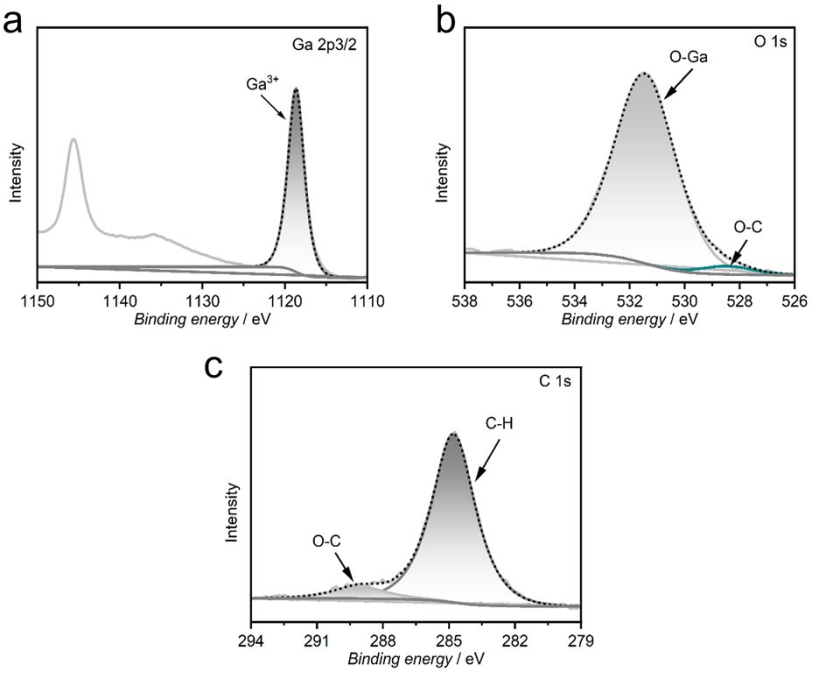

Figure S23. XPS spectra of **Ga-CO_2** (a) Ga $2p_{3/2}$, (b) O 1s and (c) C 1s.

Table S3. M-M distances of the Al-based coordination materials reported in the Cambridge Crystallographic Data Centre (CCDC) database. Surveyed using ConQuest as of June 1st, 2024.

CCDC code	Al-Al distance / Å	CCDC code	Al-Al distance / Å	CCDC code	Al-Al distance / Å	CCDC code	Al-Al distance / Å
Bridging type M−(R−COO)$_2$(X)$_1$−M							
DIJNET	3.312	CAMTET	3.281	DAZKEX	3.280	EHALOP	3.315
EFAQAH01	3.316	CAMTET01	3.285	DAZKIB	3.277	EHEJOT	3.267
EFAQAH02	3.315	CAMTOD	3.31	DAZMID	3.328	EMAGUX	3.423
HIJLEV	3.376	CAMTOD01	3.304	DEKSAR	3.165	EMAHAE	3.423
HIJMIA	3.364	CAMTOD02	3.305	DEKSEV	3.171	FEDWEU	3.325
MEZJOU	3.157	CAMTOD03	3.304	DITGUL	3.288	FEDWEU01	3.310
MEZJUA	3.162	CAMTOD04	3.301	DITHAS	3.211	FIYSAK	3.286
PIBZUY03	3.397	CAMTOD05	3.303	DITHEW	3.276	FOMMUS	3.130
RIBSAA	3.150	CAMTOD06	3.299	DITHEW01	3.267	FOMNAZ	3.266
UDUCOP	3.315	CAMVEV	3.309	DITHOG	3.242	GABWAL	3.294
UDUCOP01	3.311	CAMVOF	3.309	DITHUM	3.271	GUKVAK	3.423
UDUCOP02	3.308	CAMVUL	3.304	DITJAU	3.333	GUKVEO	3.312
UDUCOP03	3.313	CAMVUL01	3.305	DITJEY	3.279	GUKVIS	3.208
UDUCOP04	3.296	CAMWEW	3.323	DITJEY01	3.291	HAFQOW	3.301
VICNEE	3.368	CAMWIA	3.325	DITJEY02	3.353	HAFQUC	3.322
YIBHIE	3.310	CAMWOG	3.337	DITJIC	3.282	HAWMEZ	3.247
YIBHOK	3.312	CAMWUM	3.308	DITJOI	3.361	HAWMID	3.175
YIBHUQ	3.306	CAMWUM01	3.298	DITRIK	3.276	IHENIV	3.513
YIBJAY	3.310	CAMWUM02	3.285	DITROQ	3.289	INOCUM	3.344
YIBJEC	3.309	CAMXOH	3.296	DITROQ01	3.207	IZAYUG	3.317
YIBJIG	3.305	CAMXUN	3.322	DITRUW	3.279	IZAZIV	3.325
YIBJIG01	3.303	CAMYAU	3.306	DITSAD	3.295	JEKYUW	3.426
YIBJIG02	3.306	CAMYEY	3.305	DOYBEA	3.421	JIZWAS	3.312
YIBLAA	3.311	CELZIE	3.336	EFAPUA	3.318	JIZWAS01	3.310
ZIPCEK	3.329	CELZOK	3.251	EFAQAH	3.316	JIZWAS02	3.313
ZIPCIO	3.294	CELZUQ	3.31	EFAQEL	3.316	KALHAK	3.310
ZIPCUA	3.295	CEMLIS	3.316	EGELIM	3.317	KALHOY	3.309
ARURIR	3.286	CEMLOY	3.295	EGELOS	3.317	KALHUE	3.311
ARUROX	3.322	DAWJAQ	3.08	EGELUY	3.317	KALJAM	3.309
BUSPIP	3.175	DAWJUK	3.296	EGELUY01	3.311	KAPXAE	3.314
KAPXEI	3.285	OTEBEW	3.29	QOXQOM	3.317	SABVUN	3.304
KAPXIM	3.337	OTEBIA	3.296	QOXQUS	3.282	SABVUN01	3.3
KENKOE	3.176	OTEBOG	3.265	QOXRAZ	3.276	SABVUN02	3.305

CCDC code	Al-Al distance / Å	CCDC code	Al-Al distance / Å	CCDC code	Al-Al distance / Å	CCDC code	Al-Al distance / Å
KUKWAR	3.376	OTEBOG	3.276	QOXRED	3.31	SABWAU	3.288
KUKWEV	3.4	OTECEX	3.299	QOXRIH	3.289	SABWAU01	3.29
KUKWIZ	3.398	OTECIB	3.325	QOXRON	3.304	SEWPAL	3.33
KUZPUT	3.29	OTECOH	3.309	QOXSAA	3.295	TABLAN	3.434
KUZQAA	3.256	OTECUN	3.319	QOXSII	3.293	TEPJAB	3.167
LIXPOA	3.346	OTEDAU	3.305	QOXSOO	3.304	TEWZEE	3.306
LORPOA	3.313	OTEDAU	3.279	QOXSUU	3.307	TOXMUQ	3.381
LUWBUD	3.38	OTEDIC	3.284	QOXTEF	3.306	TOXNAX	3.382
MILQIJ	3.308	OTEDOI	3.287	QOXTOP	3.304	TOXNEB	3.4
MILQOP	3.321	OTEDUO	3.295	QOXTUV	3.281	TOXNIF	3.373
MUKHEI	3.328	OTEFAW	3.332	QOXVEH	3.307	UGATAA	3.317
MUZKAV	3.168	OTEFEA	3.293	QUCFOL	3.4	UGATEE	3.311
MUZKEZ	3.175	OTEFIE	3.294	QUCFUR	3.607	VABHUF	3.39
NEDTID	3.265	OTIBUQ	3.291	QUSKEX	3.334	VABJAN	3.391
NEDTOJ	3.28	OVEJUX	3.402	QUSLOI	3.313	VABLAP	3.388
NEWCAW	3.371	OYEWEW	3.178	QUSLUO	3.314	VAQTOZ	3.295
NIRPAI	3.371	OYEWIA	3.301	QUSMAV	3.32	VAQTUF	3.499
NIRPEM	3.344	OZEMIS	3.355	QUSMEZ	3.318	WAYMEQ	3.306
NIRPIQ	3.36	OZEMOY	3.409	QUSMEZ01	3.316	WAYMIU	3.28
NIRPOW	3.346	OZEMUE	3.369	QUSMID	3.305	WAYMOA	3.336
OGUJUY	3.325	PARPII	3.274	QUSMOJ	3.323	WEVYEE	3.348
OGUKAF	3.282	PIBZOS	3.29	RAWZIA	3.332	WOJJOV	3.305
OGUKEJ	3.313	PIBZUY	3.294	RAYYOI	3.307	XERJOV	3.156
OQOBUT	3.304	PICBAH	3.301	RECZUY	3.3	XERJOV01	3.244
OQOCAA	3.316	QONQAM	3.312	RIXPOF	3.316	XOCROY	3.372
OTAZUG	3.306	QONQEQ	3.327	SABVOH	3.314	XOWJEB	3.313
OTEBAS	3.291	QOXQEC	3.302	SABVOH01	3.292	XUPSAE	3.403
XUXPEO	3.267	ZESZEE	3.275	JEHWUS	3.322	WIRXOO	3.242
YABROM	3.328	ZOVHUQ	3.351	JEHXAZ	3.309	ZIPCEK01	3.308
YEYDUE	3.387	JEHWEC	3.33	JEHXIH	3.289	YUQDUL	3.276
YEYDUE	3.258	JEHWIG	3.305	JEHXON	3.325	JEHWOM	3.306
JEHXUT	3.31						

CCDC code	Al-Al distance / Å	CCDC code	Al-Al distance / Å	CCDC code	Al-Al distance / Å	CCDC code	Al-Al distance / Å
Bridging type M−(R−COO)$_1$(X)$_2$−M							
ZIPCEK	2.871	FICBUS	2.878	JEHXAZ	2.851	QUSKIB	2.869
BUSQIQ	2.83	FICCAZ	2.85	JEHXIH	2.899	QUSLOI	2.847
DAWJAQ	2.84	JEHWUS	2.853	JEHXON	2.862	QUSLUO	2.85
DAWJUK	2.867	DESLAS	2.893	JEHXUT	2.843	QUSMAV	2.855
DESHAO	2.835	DESLAS	2.985	KIKNOL	2.828	QUSMEZ	2.849
DESKUL	2.868	DESLEW	2.882	KIKNUR	2.959	QUSMEZ01	2.856
DESHES	2.873	DESLEW	2.965	KIKPED	2.831	QUSMID	2.857
DESHIW	2.857	DESLIA	2.867	MIJMOL	2.82	QUSMOJ	2.866
DESHOC	2.844	IZAYEQ	2.863	MIJMUR	2.816	UTABOJ	2.886
DESHUI	2.854	IZAYUG	2.844	ZIPCEK01	2.874	UTABUP	2.883
DESJAQ	2.873	IZAZIV	2.833	DESLIA	2.978	UTACAW	2.882
DESJEU	2.868	IZEBEX	2.85	DESLOG	2.863	UTACOK	2.874
DESJIY	2.867	MUKHUY	2.86	TEWZEE	2.862	WAKHAU	2.798
DESJOE	2.858	NEMQEE	2.792	JEHWEC	2.867	WAKHAU01	2.825
DESJUK	2.853	NEMQII	2.785	JEHWIG	2.84	QUSKEX	2.86
DESKOF	2.893	OTEBIA	2.866	JEHWOM	2.862	YABROM	2.846
RUPNEW	2.887						

Table S4. M-M distances of the Ga-based coordination materials reported in the Cambridge Crystallographic Data Centre (CCDC) database. Surveyed using ConQuest as of June 1st, 2024.

CCDC code	Ga-Ga distance / Å	CCDC code	Ga-Ga distance / Å	CCDC code	Ga-Ga distance / Å	CCDC code	Ga-Ga distance / Å
Bridging type M−(R−COO)$_2$(X)$_1$−M							
YUWBUO	3.376	QOVWUU01	3.371	VIGMIL	3.358	DUDGOB	3.328
QOZYAG	3.383	VIGJII	3.364	VIGMOR	3.33	DUDGUH	3.335
HIJKUK	3.436	VIGJOO	3.346	VIGMUX	3.354	OTAQAD	3.349
HIJLAR	3.431	VIGJUU	3.360	VIGNAE	3.357	DUDGUH	3.335
LOQLIN02	3.355	VIGKAB	3.360	VIGSEN	3.371	DUDGUH	3.335
LOQLIN03	3.352	VIGKEF	3.359	VIGSIR	3.376	OVEKIM	3.419
LOQLIN04	3.352	VIGKIJ	3.359	AGEDIC	3.420	OVEKOS	3.366
LOQLIN05	3.349	VIGKOP	3.358	ASAKUC	3.432	OVEKUY	3.365
LOQLIN06	3.379	VIGKUV	3.358	COMDOY	3.367	PARPUU	3.390
LOQLIN07	3.371	VIGLAC	3.358	DENLUG	3.308	PEDWON	3.318
LOQLIN08	3.369	VIGLEG	3.359	DONNAW	3.361	QAWBUN	3.385

CCDC code	Ga-Ga distance / Å	CCDC code	Ga-Ga distance / Å	CCDC code	Ga-Ga distance / Å	CCDC code	Ga-Ga distance / Å
LOQLIN09	3.371	VIGLIK	3.360	DONNAW01	3.374	QOVWOO	3.341
LOQLIN10	3.370	VIGLOQ	3.360	DONNEA	3.363	QOVWOO01	3.336
LOQLIN11	3.370	VIGMAD	3.361	DONNIE	3.364	QOZYAG	3.382
QOVWOO02	3.336	VIGMEH	3.357	DOTTEM	3.372	QUFCUS	3.233
YATROD	3.510	YEDVIQ	3.350				
Bridging type M−(R−COO)$_1$(X)$_2$−M							
CESGAJ	2.962	CESGEN	2.927				
Bridging type M−(X)$_2$−M							
ALAGEA01	3.097	QUDBIA	3.013	TEVPAL	3.145	VIQROE	3.080
QIZHAJ	3.081	TEVNIR	3.042	TEVPEP	3.055	YELBEW	3.070
PAFJOW	3.037						

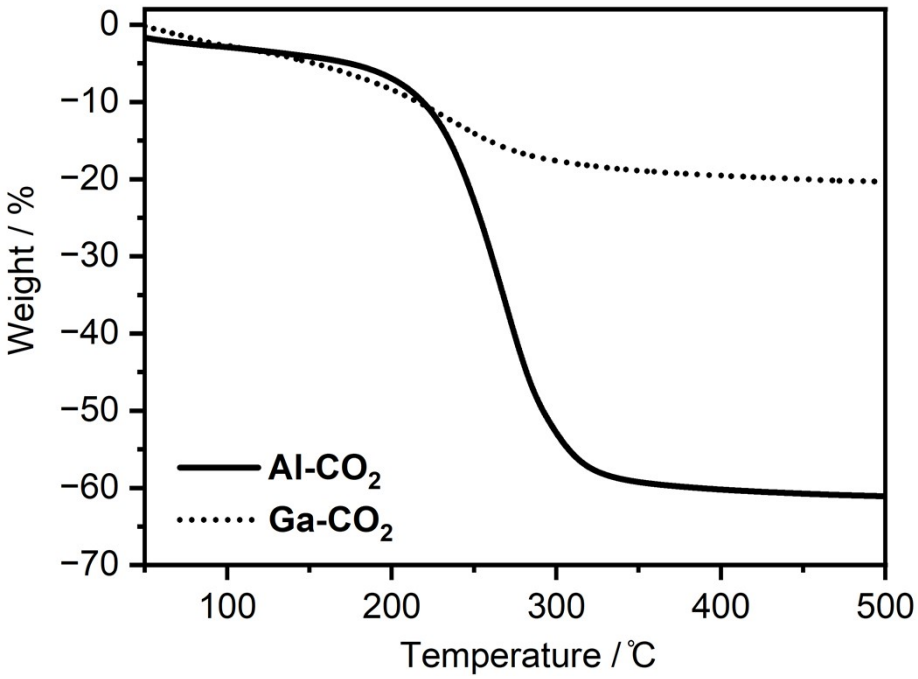

Figure S24. TGA curves of **Al-CO$_2$** and **Ga-CO$_2$** under N_2.

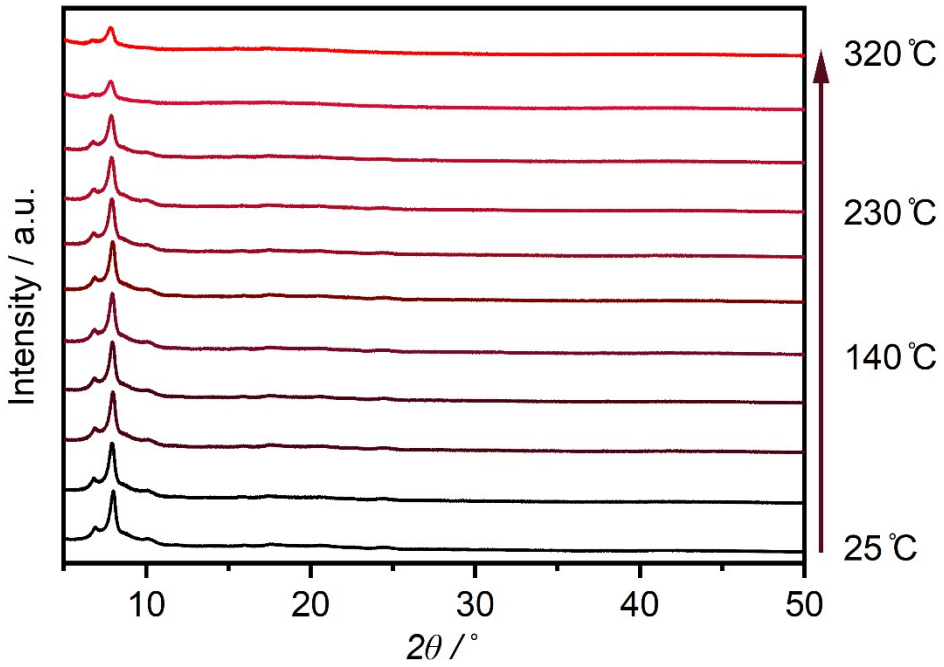

Figure S25. Variable-temperature synchrotron PXRD patterns of **Al-CO_2**.

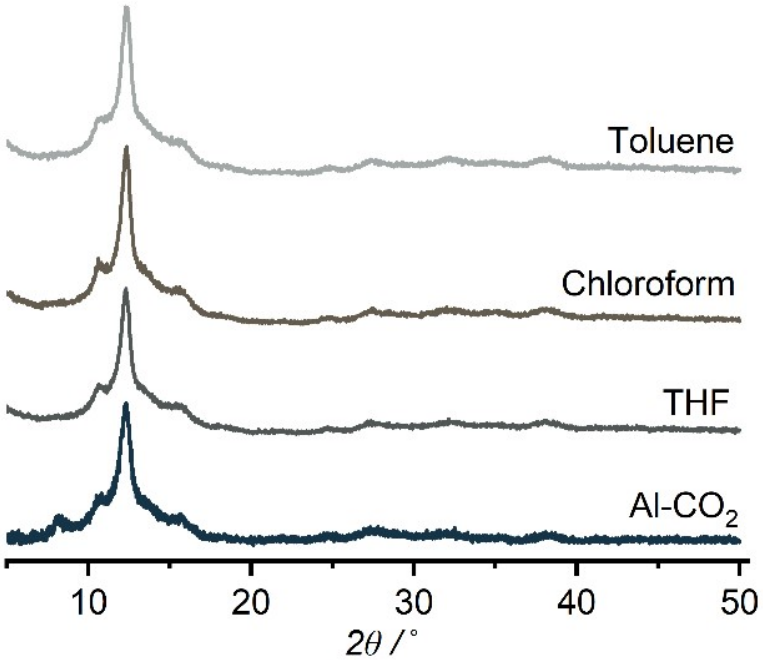

Figure S26. PXRD patterns of **Al-CO_2** after soaking in solvent 24 hours; THF, chloroform, and toluene.

CO_2 cycloaddition reaction; CO_2 conversion calculation

Conversion (%) calculated from the integral values (I) of proton in the starting reagents and products using $CDCl_3$ as a solvent.[6, 7]

$$\textbf{\% Conversion} = (I_{Hb'} \times 100) / (I_{Hb} + I_{Hb'})$$

I_{Hb} = Integral of ^{1}Hb peak
$I_{Hb'}$ = Integral of ^{1}Hb' peak

Epoxide	δH ($CDCl_3$)(epoxide, ^{1}Hb)	δH ($CDCl_3$)(epoxide, ^{1}Hb')
Epichlorohydrin	2.67	4.40
Styrene oxide	2.78	4.31

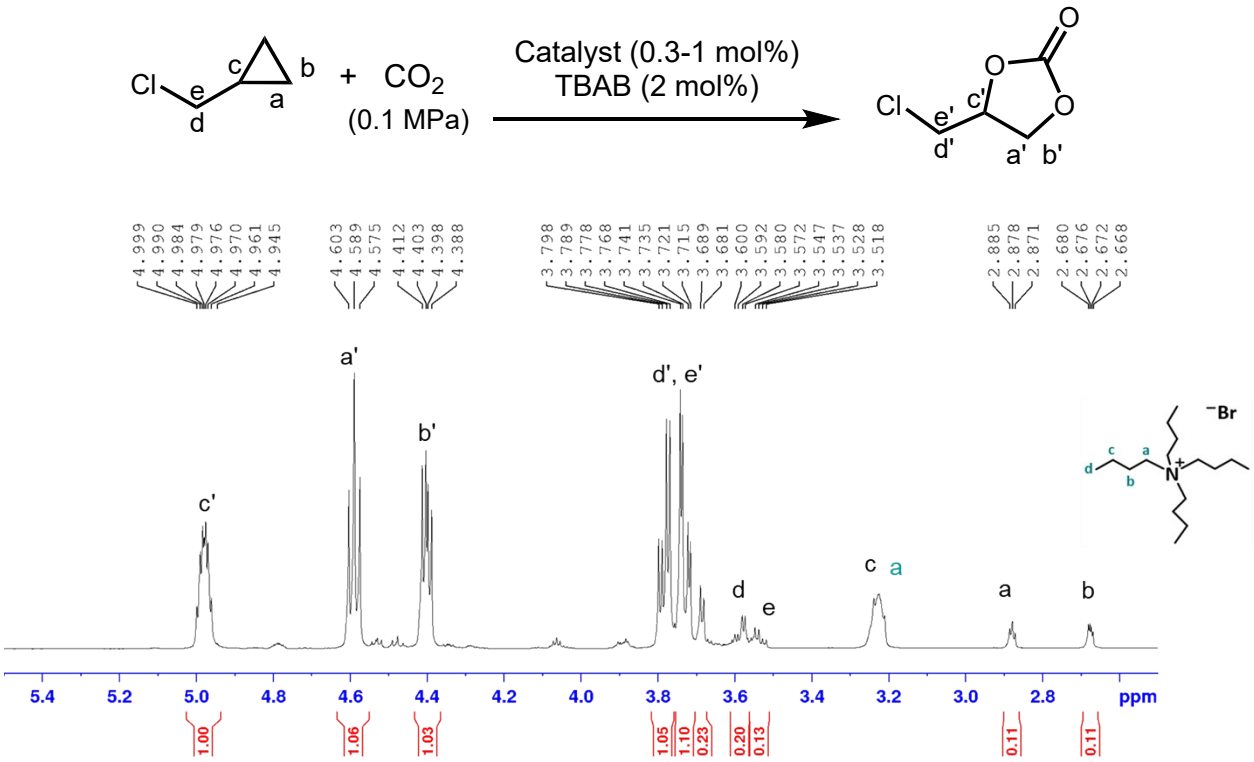

Figure S27. ^{1}H NMR ($CDCl_3$) spectrum of cycloaddition of CO_2 to CPC by using 1 mol% of **Al-CO_2** (0.1 MPa of CO_2, 30 °C, 48 h).

Table S5. Catalytic performance and reaction conditions of literature and ***M*-CO_2** for CO_2 cycloaddition with ECH at mild conditions.

Catalyst	CO_2 pressure	Temp / °C	Time / h	Catalyst / mol%	TBAB / mol%	Conversion / %	TON	TOF / h^{-1}	Ref.
Cu-MOF	0.1 MPa	80	12	0.25	1.25	82	320	26.7	8
$Cu_2(O_2C)_4$	0.1 MPa	70	16	0.40	0.20	>99	-	-	7
	0.1 MPa	70	24	0	0.31	43	-	-	9
Zn-MOF	0.1 MPa	70	24	0.45	0.31	98	217	9.0	
Zn-MOF	0.1 MPa	30	24	0.45	0.31	53	118	4.9	
Zn-MOF	0.1 MPa	40	24	0.44	1	>99	225	9	10
Zn-URJC-8	1.2 MPa	25	24	1.0	5	91	-	-	11
	0.1 MPa	25	24	1.5	5	86	-	-	
Al-fumarate	1.0 MPa	50	6	20 mg	2	96	-	-	12
Ba-MOF	0.1 MPa	RT	48	0.5	2	90.2	180	3.8	13
TMOF (Cu-MOF)	0.1 MPa	RT	48	1	10	92	-	-	14
Ni-MOF	0.1 MPa	60	24	0.05	1	97	39	6.5	15
Co-MOF	0.1 MPa	RT	48	0.08	7.5	74.2	1020[a]	21.3[a]	16
	0.1 MPa	30	12	0	2	23.8	-	-	This work
	0.1 MPa	30	24	0	2	39.5 ± 4.3	-	-	This work
	0.1 MPa	30	48	0	2	67.5 ± 3.1	-	-	This work
	0.1 MPa	30	72	0	2	88.8	-	-	This work
Al-CO_2	0.1 MPa	30	24	0.3	2	49.8	176	7.3	This work
Al-CO_2	0.1 MPa	30	24	0.5	2	54.2 ± 4.3	108	4.5	This work
Al-CO_2	0.1 MPa	30	48	0.5	2	81.5 ± 5.5	163	3.4	This work
Al-CO_2	0.1 MPa	30	12	1.0	2	26.3	26	2.2	This work
Al-CO_2	0.1 MPa	30	24	1.0	2	55.6 ± 6.0	56	2.3	This work
Al-CO_2	0.1 MPa	30	48	1.0	2	94.4 ± 5.8	94	2.0	This work
Al-CO_2	0.1 MPa	30	72	1.0	2	97.9	98	1.4	This work
Ga-CO_2	0.1 MPa	30	24	0.5	2	55.8 ± 4.4	112	4.7	This work
Ga-CO_2	0.1 MPa	30	48	0.5	2	81.8 ± 7.4	164	3.4	This work
Ga-CO_2	0.1 MPa	30	12	1.0	2	32.2	32	2.7	This work
Ga-CO_2	0.1 MPa	30	24	1.0	2	61.2 ± 3.9	61	2.6	This work
Ga-CO_2	0.1 MPa	30	48	1.0	2	91.6 ± 0.1	92	1.9	This work
Ga-CO_2	0.1 MPa	30	72	1.0	2	98.4	98	1.4	This work

TON calculated by N (mmol of Product)/N (mmol of catalyst)
TOF = TON/reaction time (h)
[a]TON/TOF calculated using mmol of active site

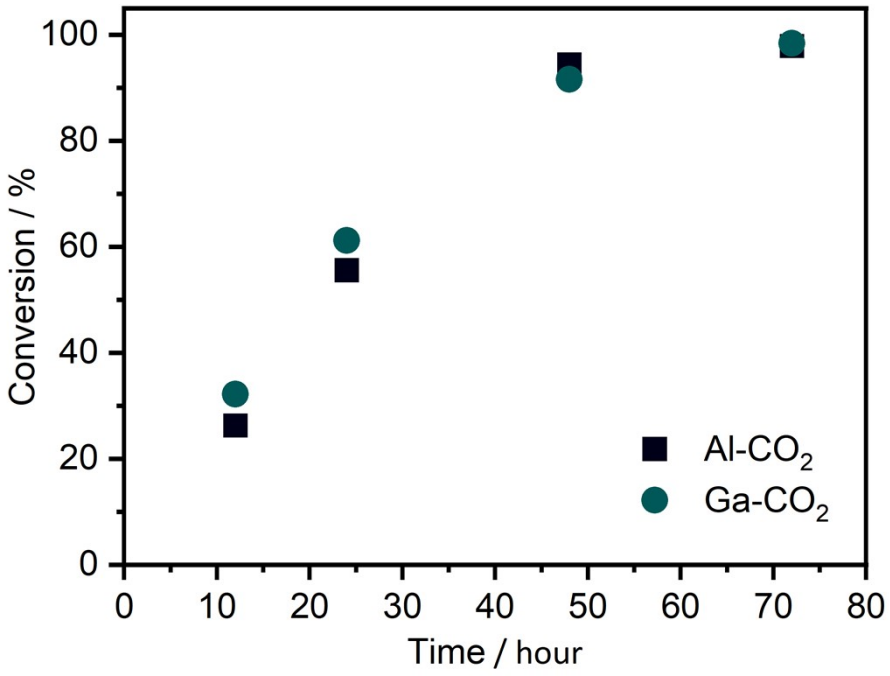

Figure S28. Time-course of conversion of ECH into CPC with the presence of ***M*-CO$_2$** (1.0 mol%) and TBAB (2.0 mol%) at 30 °C under 0.1 MPa of CO_2.

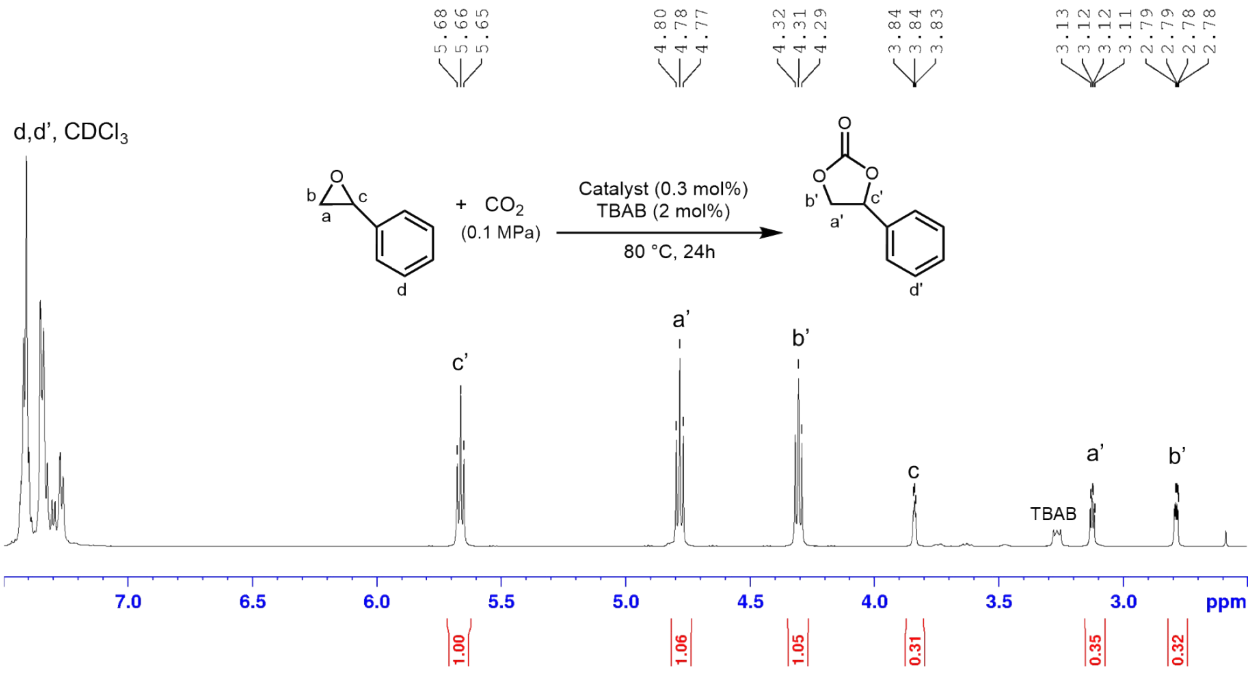

Figure S29. ^{1}H NMR ($CDCl_3$) spectrum of cycloaddition of CO_2 to styrene carbonate by using 0.3 mol% of **Al-CO$_2$** (0.1 MPa of CO_2, 80 °C, 24 h).

Table S6. Catalytic performance and reaction conditions of literature and **Al-CO_2** for CO_2 cycloaddition with styrene oxide at mild conditions.

Catalyst	CO_2 pressure	Temp / °C	Time / h	Catalyst / mol%	TBAB / mol%	Conversion / %	TON	TOF / h^{-1}	Ref.
Zn-MOF	0.1 MPa	70	24	0.45	0.31	82	181	7.5	9
NUC-54(Cu)	0.1 MPa	60	8	0.3	4	97	323	40	17
FCG-1a	0.1 MPa	100	12	0.35	0.35	97	315	26.3	18
Cu-URJC-8	1.2 MPa	30	24	1	4	47	-	-	19
Cu-MOF	0.1 MPa	80	12	0.25	1.25	81	324	27	8
n-SU-101	0.1 MPa	80	7	0.32	1	1.3	-	-	20
n-SU-101	0.3 MPa	80	7	0.32	1	96.6	302	43.1	
Co-MOF	0.1 MPa	RT	48	0.08	7.5	51.8	712[a]	14.8[a]	16
	0.1 MPa	70	12	0	2	37.9	-	-	This work
Al-CO_2	0.1 MPa	70	12	0.3	2	49.8	175	14.6	This work
Al-CO_2	0.1 MPa	80	12	0.3	2	52.4	185	15.4	This work
Al-CO_2	0.1 MPa	80	24	0.3	2	76.3	269	11.2	This work

TON calculated by N (mmol of Product)/N (mmol of catalyst)
TOF = TON/reaction time (h)
[a]TON/TOF calculated using mmol of active site

Table S7. Conversion and metal leaching on the supernatant after the reactions of recycling runs of ECH-CO_2 cycloaddition. (condition: catalyst 1 mol%, TBAB 2 mol%, T = 30 °C, t = 48 h and P = 0.1 MPa).

Catalyst	**Cycle**	**Conversion / %**	**Metal leaching / ppm** by ICP-OES
Al-CO_2	1st	94.4 ± 5.8	0.20 ± 0.15
	2nd	91.1 ± 10.7	0.14 ± 0.15
	3rd	93.9 ± 7.6	0.33 ± 0.18
Ga-CO_2	1st	91.6 ± 0.1	0.09 ± 0.02
	2nd	89.2	0.07 ± 0.02
	3rd	93.9 ±0.8	0.07 ± 0.03

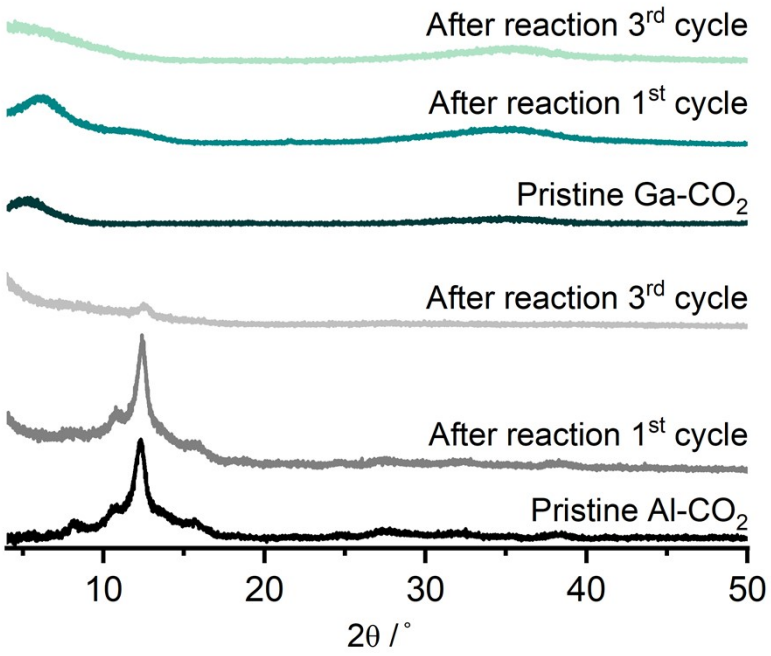

Figure S30. PXRD patterns of ***M*-CO_2** and ***M*-CO_2** after CO_2 cycloaddition with ECH.

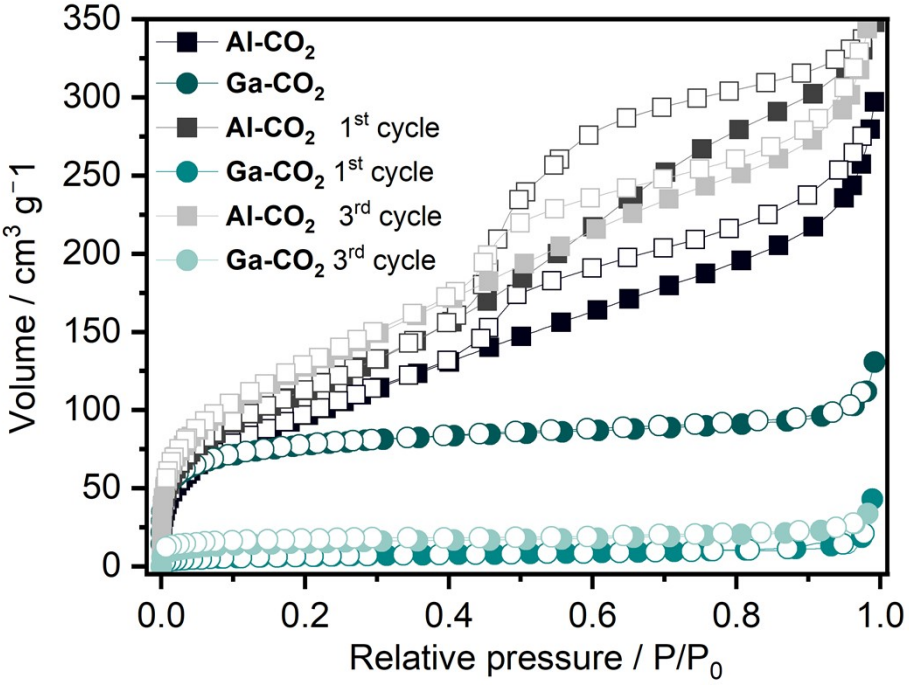

Figure S31. N_2 adsorption isotherms of ***M*-CO_2** at 77 K before and after CO_2 cycloaddition.

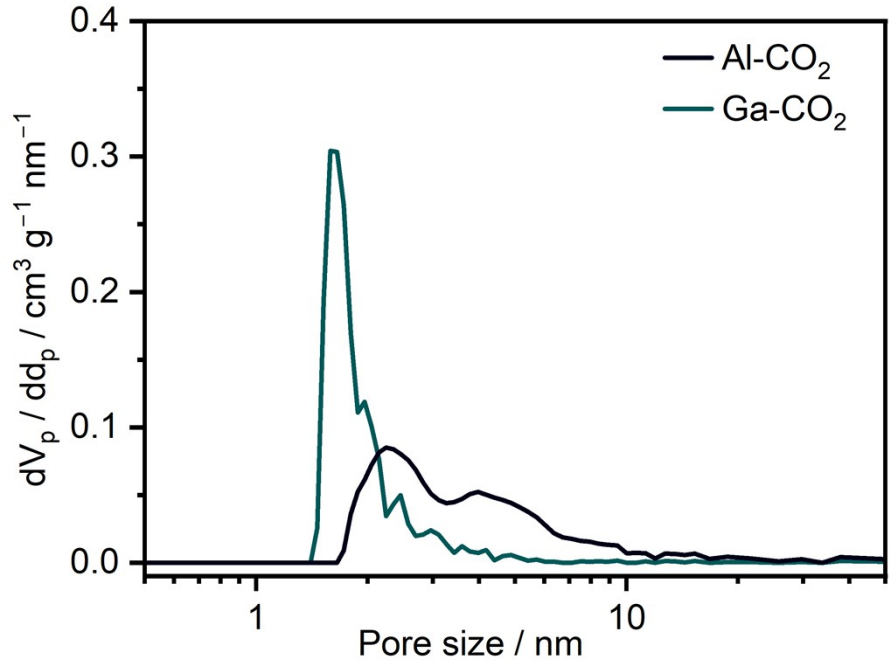

Figure S32. Pore size distribution of **Al-CO_2** and **Ga-CO_2**.

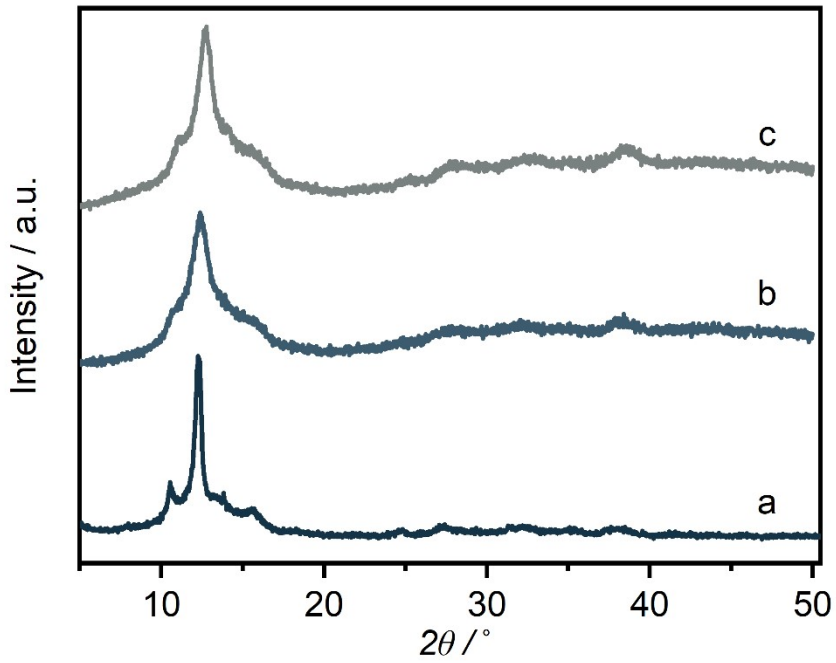

Figure S33. PXRD patterns of **Al-CO_2** as (a) powder, (b) hand-grinded powder, and (c) monolith

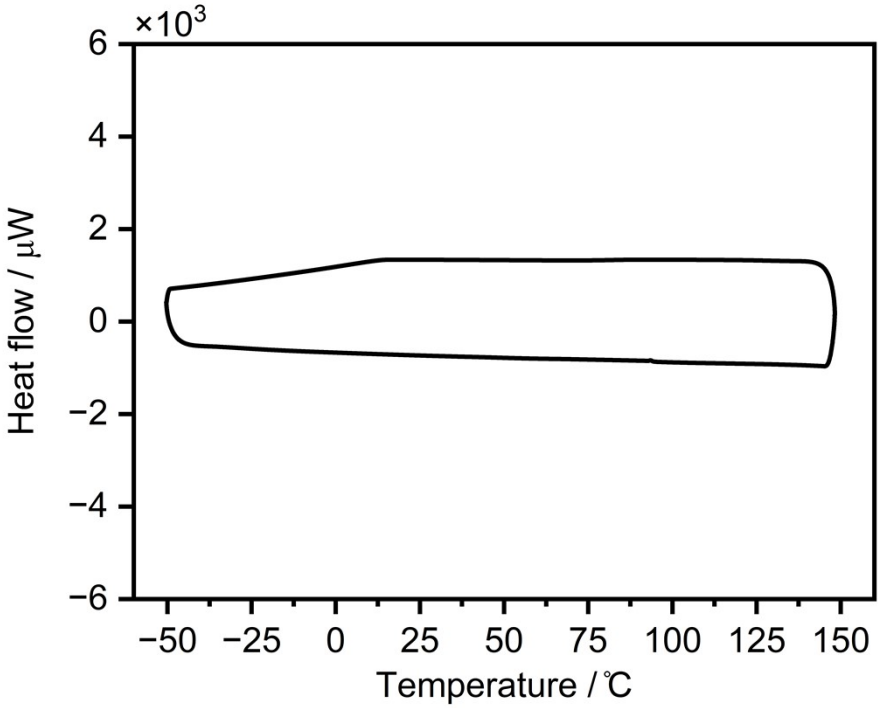

Figure S34. The 2nd cycle of DSC profile of ground **Al-CO_2** powder.

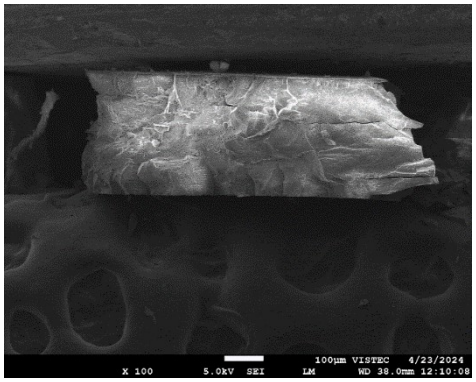

Figure S35. Cross-sectional SEM image of **Al-CO_2** monolith.

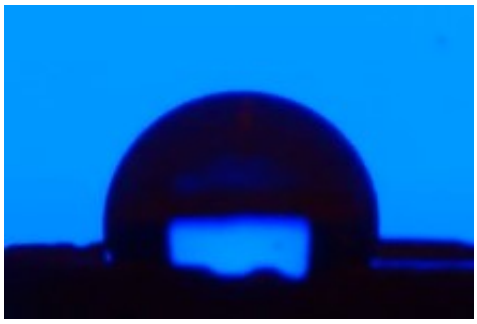

Figure S36. Photo of water droplet from contact angle measurement of **Ga-CO_2** monolith.

Table S8. Gas adsorption properties of ***M*-CO_2** before and after hot-pressing.

		S_{BET} ($m^2\ g^{-1}$)	Volume ($cm^3\ g^{-1}$)	d_p (nm)	Uptake at P/P_0 of 1.0 ($cm^3\ g^{-1}$)	Reduction of gas uptake (%)
N_2 adsorption properties at 77 K						
Al-CO_2	Powder	362.7	0.49	2.4	297.1	94.2
	Monolith	31.1	0.03	2.6	17.2	
Ga-CO_2	Powder	277.2	0.24	1.6	130.7	85.4
	Monolith	56.0	0.04	1.8	19.14	
CO_2 adsorption properties at 195 K						
Al-CO_2	Powder	168.41	0.31	0.34	98.6	81.4
	Monolith	48.0			18.3	
Ga-CO_2	Powder	221.4	0.19	0.34	68.0	83.2
	Monolith	40.7			11.4	
H_2 adsorption properties at 77 K						
Al-CO_2	Powder				27.5	21.8
	Monolith				21.5	
Ga-CO_2	Powder				32.0	63.4
	Monolith				11.7	

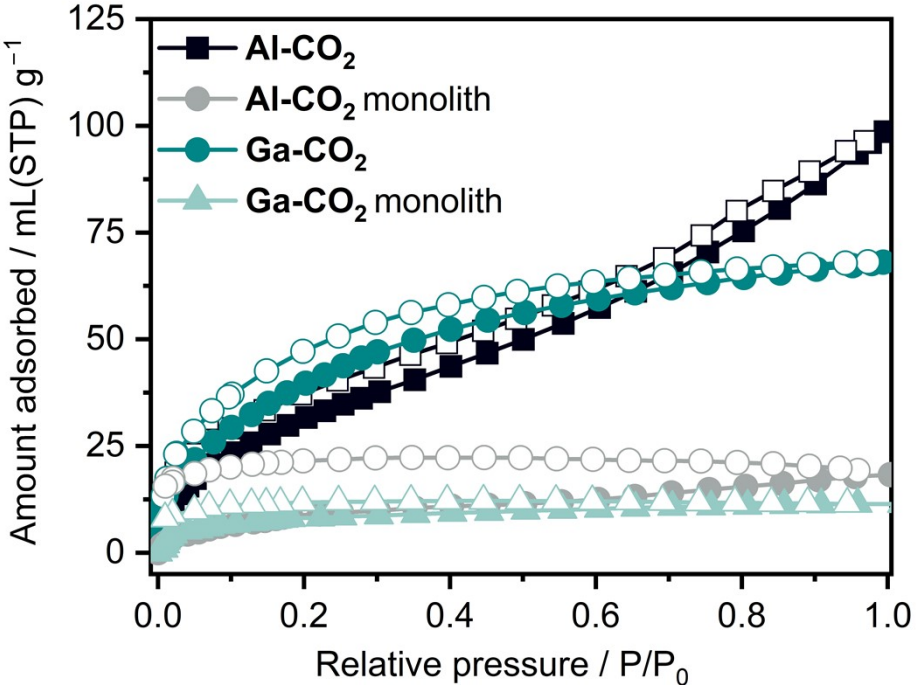

Figure S37. CO_2 adsorption isotherms of **Al-CO_2** and **Ga-CO_2** as powder and monoliths at 195 K.

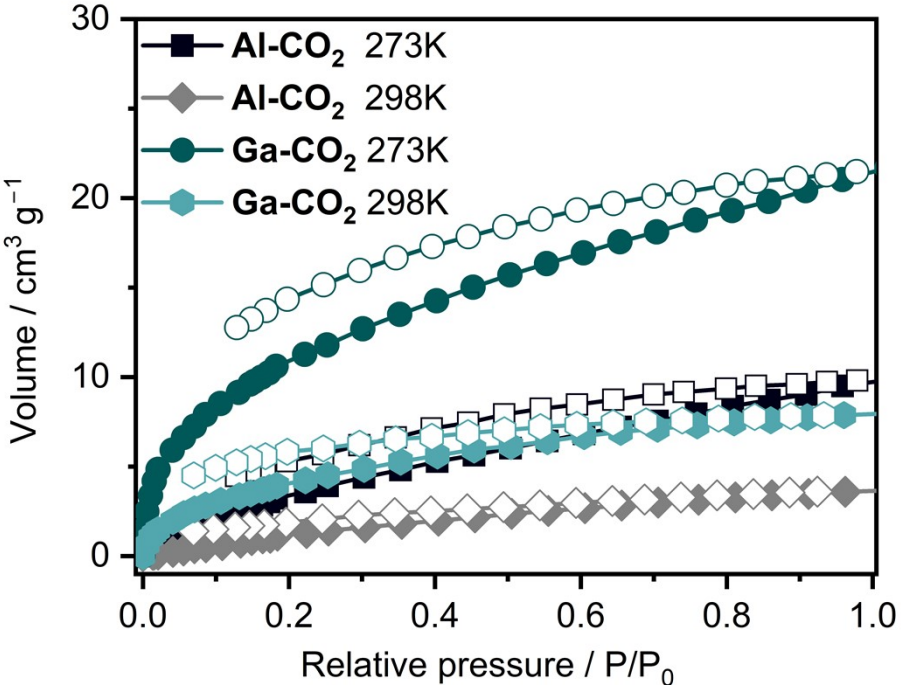

Figure S38. CO_2 adsorption isotherms of **Al-CO_2** and **Ga-CO_2** powder at 273 and 298 K.

Reference

1. C. Hennig, A. Ikeda-Ohno, W. Kraus, S. Weiss, P. Pattison, H. Emerich, P. M. Abdala and A. C. Scheinost, *Inorg. Chem.*, 2013, **52**, 11734-11743.
2. A. S. Jbara, Z. Othaman, A. A. Ati and M. A. Saeed, *Mater. Chem. Phys.*, 2017, **188**, 24-29.
3. B. Cheng and E. T. Samulski, *J. Mater. Chem.*, 2001, **11**, 2901-2902.
4. V. N. Krasil'nikov, A. P. Tyutyunnik, I. V. Baklanova, A. N. Enyashin, I. F. Berger and V. G. Zubkov, *CrystEngComm*, 2018, **20**, 2741-2748.
5. Y.-Q. Tian, Y.-M. Zhao, H.-J. Xu and C.-Y. Chi, *Inorg. Chem.*, 2007, **46**, 1612-1616.
6. S. Kaewsai, S. Del Gobbo and V. D'Elia, *ChemCatChem*, 2024, **16**, e202301713.
7. A. K. Gupta, N. Guha, S. Krishnan, P. Mathur and D. K. Rai, *J. CO2 Util.*, 2020, **39**, 101173.
8. X. Yu, J. Gu, X. Liu, Z. Chang and Y. Liu, *Inorg. Chem.*, 2023, **62**, 11518-11527.
9. A. Eskemech, H. Chand, A. Karmakar, V. Krishnan and R. R. Koner, *Inorg. Chem.*, 2024, **63**, 3757-3768.
10. Z. A. K. Khattak, N. Ahmad, H. A. Younus, H. Ullah, B. Yu, K. S. Munawar, M. Ashfaq, M. Yaseen, M. Danish, M. Al-Abri, R. AlHajri and F. Verpoort, *Catal. Sci. Technol.*, 2024, **14**, 1888-1901.
11. J. Tapiador, P. Leo, A. Rodríguez-Diéguez, D. Choquesillo-Lazarte, G. Calleja and G. Orcajo, *Catal. Today*, 2022, **390-391**, 230-236.
12. H. S. Kim, K. Yu, P. Puthiaraj and W.-S. Ahn, *Micropor. Mesopor. Mater.*, 2020, **306**, 110432.
13. X.-Y. Li, L.-N. Ma, Y. Liu, L. Hou, Y.-Y. Wang and Z. Zhu, *ACS Appl. Mater. Interfaces.*, 2018, **10**, 10965-10973.
14. G. Zhang, G. Wei, Z. Liu, S. R. J. Oliver and H. Fei, *Chem. Mater.*, 2016, **28**, 6276-6281.
15. J. Li, W.-J. Li, S.-C. Xu, B. Li, Y. Tang and Z.-F. Lin, *Inorg. Chem. Commun.*, 2019, **106**, 70-75.
16. X. Zhang, J. Wang, Y. Bian, H. Lv, B. Qiu, Y. Zhang, R. Qin, D. Zhu, S. Zhang, D. Li, S. Wang, W. Mai, Y. Li and T. Li, *J. CO_2 Util.*, 2022, **58**, 101924.
17. H. Chen, T. Zhang, S. Liu, H. Lv, L. Fan and X. Zhang, *Inorg. Chem.*, 2022, **61**, 11949-11958.
18. P. P. Mondal, S. Sarkar, M. Singh and S. Neogi, *ACS Sustain. Chem. Eng.*, 2024, **12**, 15432-15446.
19. J. Tapiador, P. Leo, F. Gándara, G. Calleja and G. Orcajo, *J. CO_2 Util.*, 2022, **64**, 102166.
20. J. L. Obeso, J. G. Flores, C. V. Flores, V. B. López-Cervantes, V. Martínez-Jiménez, J. A. de los Reyes, E. Lima, D. Solis-Ibarra, I. A. Ibarra, C. Leyva and R. A. Peralta, *Dalton Trans.*, 2023, **52**, 12490-12495.